Frontiers in Health Informatics
ISSN-Online: 2676-7104
www.healthinformaticsjournal.com
2024; Vol 13: Issue 7
Open Access

SYNTHESIS, CHARACTERIZATION, AND BIOLOGICAL EVALUATION OF BENZOTHIAZOLE-CONJUGATED PYRIMIDINES DERIVED FROM 2-AMINOACETOPHENONE AS POTENTIAL ANTITUBERCULAR AND CYTOTOXIC AGENTS.

Koduru Aparna Surya Mani[1*], Dr. Atla Srinivasarao[2], Dr. Y. Rajendera Prasad[3], Dr. S.Arun Satyadev[4], Dr. Lagu Surendra Babu [5]

1. Avanthi Institute Of Pharmaceutical Sciences, Vizianagaram, Andhra Pradesh, India
2. Shri Vishnu College Of Pharmacy, Bheemavaram, Kovvada, Andhra Pradesh, India
3. Andhra University College Of Pharmaceutical Sciences, Visakhapatanam, Andhra Pradesh, India
4. Andhra University College Of Pharmaceutical Sciences, Visakhapatanam, Andhra Pradesh, India
5. Aadikavi Nanaya University, Rajhmundry, Andhra Pradesh, India.

Abstract

The present study aims to synthesize and characterize benzothiazole conjugated pyrimidines as potential anti-tubercular and anti-cancer agents.We have attempted to synthesize and characterize a series of benzothiazole analogs from the key intermediate 1-(2-aminobenzo[d]thiazol-4-yl)ethanone (I). In this process we have synthesized 14 new hybrids (PR1-PR14) were appropriately established by melting point, IR,NMR, mass spectroscopic and analytical data. These compounds were further subjected to their *in vitro* antitubercular activity using *Mycobacterium tuberculosis* H37Rv strain and to evaluate their *in vitro* cytotoxicity potential using colon and breast cancer cell lines. Finally, to identify the '*in silico* hit' against validated anticancer and antitubercular drug targets for further exploitation using molecular docking simulations molecular modeling studies were performed to ensure the anti-tubercular and cytotoxic activity of the compounds to explore their enzymatic inhibitory activities.

Key words: Benzothiazole, Pyrimidines, anticancer activity, antitubercular activity.

Introduction

Tuberculosis (TB) and cancer continue to pose significant global health challenges in the 21st century[2]. TB, which is caused by Mycobacterium tuberculosis (Mtb), leads to more than 1.5 million fatalities each year, with the emergence of drug-resistant forms (MDR-TB and XDR-TB) further complicating treatment options and increasing mortality rates. In parallel, cancer is responsible for nearly 10 million deaths annually, influenced by factors such as genetic alterations, environmental carcinogens, and an aging demographic. Despite progress in treatment modalities including chemotherapy, radiotherapy, and immunotherapy, both conditions face obstacles such as drug resistance, systemic toxicity, and a lack of targeted therapies[1]. These issues highlight the pressing need for the development of innovative chemical entities that possess dual therapeutic capabilities to meet unmet clinical demands.

Heterocyclic compounds have consistently played a pivotal role in drug discovery, attributed to their structural variety, bioavailability, and ability to engage with biological targets. Among these compounds, benzothiazoles and pyrimidines are particularly notable for their extensive pharmacological activities. Benzothiazoles, which feature a fused benzene and thiazole ring, demonstrate properties such as antimicrobial, anticancer, anti-inflammatory, and antitubercular effects. Prominent examples include riluzole, utilized in the treatment of ALS, and Frentizole, an immunosuppressant[3]. Pyrimidines, characterized by their six-membered aromatic rings containing two nitrogen atoms, are essential for nucleic acid synthesis and serve as foundational structures for antiviral, anticancer, and antimalarial medications, such as 5-fluorouracil and zidovudine. The combination of benzothiazole and pyrimidine components presents a strategic avenue for the development of hybrid molecules that can leverage the pharmacological advantages of heterocycles, potentially addressing

resistance mechanisms and improving therapeutic outcomes.

2-Aminoacetophenone[4] serves as a significant precursor in organic synthesis and has become increasingly important in medicinal chemistry due to its utility in the formation of heterocyclic structures. The presence of amino and ketone groups facilitates its transformation into various derivatives, including benzothiazoles, pyrimidines, and chalcones, which often exhibit improved bioactivity. For example, benzothiazoles derived from 2-aminoacetophenone have shown strong antitubercular properties by inhibiting key mycobacterial enzymes such as InhA and cytochrome P450. Likewise, pyrimidine derivatives obtained from 2-aminoacetophenone have demonstrated cytotoxic effects by interfering with DNA replication and triggering apoptosis in cancer cells. The integration of these pharmacophores into a unified molecular framework—specifically, 2-aminoacetophenone-derived benzothiazole-pyrimidine hybrids—presents an innovative approach to leverage multitarget mechanisms, potentially providing therapeutic solutions for both tuberculosis and cancer.

Objectives

1. Synthesis of 2-Aminoacetophenone-Derived Benzothiazole-Pyrimidine Hybrids

Develop a library of hybrids by varying substituents on the benzothiazole (e.g., -Cl, -OCH3) and pyrimidine (e.g., -NH2, -SCH3) moieties. .

2. Antitubercular Evaluation

-Primary Screening: Test compounds against Mtb H37Rv (ATCC 27294) using the Microplate Alamar Blue Assay (MABA).[5]

- MIC Determination: Identify minimum inhibitory concentrations for active hybrids (MIC ≤10 µg/mL considered promising).
- Resistant Strains: Evaluate efficacy against MDR-TB and XDR-TB clinical isolates.
- Cytotoxicity Check: Assess toxicity toward Vero cells (CC50 >100 µg/mL desirable).

3. Cytotoxic Activity Profiling

- Cell Lines: Screen hybrids against breast (MDA-MB-231), and colon (HCT-116) cancer cells via MTT assay.

-Selectivity Index (SI): Compare IC50 values in cancer vs. normal (HEK-293) cells (SI >3 indicates selectivity).

4. Structure-Activity Relationship (SAR) Analysis

- Correlate substituent effects (electron-withdrawing/donating groups, steric bulk) with bioactivity.
- Identify critical pharmacophoric features (e.g., hydrogen bond donors, aromatic π-systems).
- Intercalate DNA (UV-Vis titration, ethidium bromide displacement).

5. In Silico Studies

-Molecular Docking: Predict binding modes with Mtb InhA (PDB: 2NSD) and human thymidylate synthase (PDB: 1JU6).

Method

The preparation of benzothiazole-linked chalcones and benzothiazole-linked pyrimidines (PR1-PR14) adheres to the reaction sequence detailed below, with the individual physical properties of each compound provided. The principal intermediate in this investigation, 1-(2-aminobenzo[d]thiazol-4-yl)ethanone (I), was synthesized from 2-aminoacetophenone (2.0 g, 14.8 mmol) and potassium thiocyanate (3.9 g, 52.0 mmol) in glacial acetic acid at a temperature of 27.5 ± 2.5°C. Subsequently, liquid bromine (2.6 g, 16.3 mmol) was added dropwise to the mixture while ensuring the temperature remained below 8°C for a duration of 160-180 minutes. Following the completion of the bromine addition, the reaction mixture was stirred, and its progress was monitored

via thin-layer chromatography (TLC). Upon completion of the reaction, as evidenced by the disappearance of the starting material, the solids were filtered, washed with glacial acetic acid, and subsequently with water. The filtrate was then diluted with 300 mL of warm water, neutralized to a pH of 6.5-7.5 using ammonia (as measured with a pH meter), and allowed to cool overnight in a refrigerator to facilitate product precipitation. The resulting solid was poured onto crushed ice, filtered under vacuum, washed with cold water, and dried. The dried residue was treated with activated carbon for decolorization and recrystallized in ethanol.

The intermediate (I) underwent a Claisen-Schmidt condensation[6] with various aromatic or heteroaromatic aldehydes in the presence of potassium hydroxide as the base and ethanol as the solvent, yielding the corresponding benzothiazole-linked chalcones[7] in good yields.

The chalcones were subsequently employed to synthesize benzothiazole-linked pyrimidines through a reaction with guanidine hydrochloride in an alkaline environment (pyridine) at reflux temperatures for a duration of 5 to 8 hours. The progress of the reaction was monitored via thin-layer chromatography (TLC) utilizing silica gel-G. Upon completion of the reaction, the mixture was poured onto crushed ice while stirring continuously. The resulting solid was then filtered, dried, and purified through column chromatography on silica gel, employing a combination of ethyl acetate and hexane as the mobile phase. The final pyrimidine derivatives (PR1-PR14) were acquired as fine powders ranging from light to bright yellow.

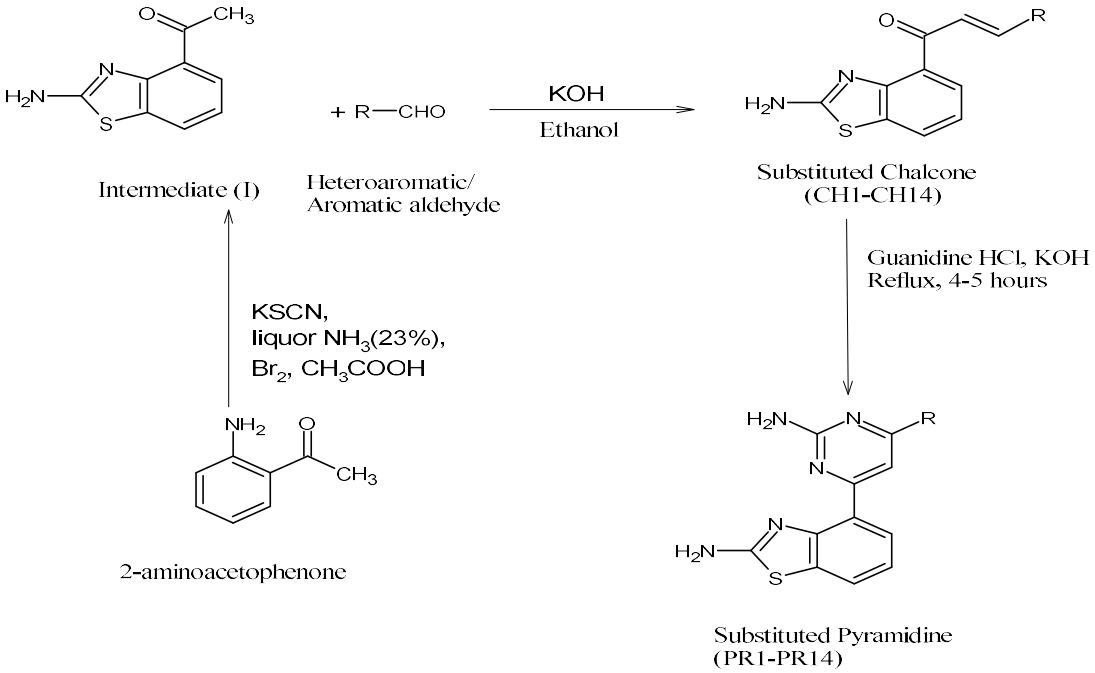

Scheme 1: Reaction pathway for the synthesis of chalcones linked to benzothiazole and pyrimidines associated with benzothiazole (PR1-PR14).

A solution of 1-(2-aminobenzo[d]thiazol-4-yl)-3-(substituted)prop-2-en-1-ones (0.005 mol) in ethanol was reacted with guanidine hydrochloride (0.005 mol) in the presence of a catalytic amount of potassium hydroxide (5-6 drops) in absolute ethanol (30 ml) at reflux temperature using a water bath for a duration of 5-6 hours. Following this, the solvent was removed under vacuum, and crushed ice was added to the resulting residue,

which was then mixed thoroughly, leading to the formation of a bright yellow solid. This solid was subsequently filtered under vacuum, dried, and purified through column chromatography, yielding a light yellow solid. The compounds 4-(2-amino-6-(substituted)pyrimidin-4-yl)benzo[d]thiazol-2-amines PR1-PR14 were produced in good yield. All synthesized compounds, as illustrated in Fig. 1.2, were characterized using spectroscopic techniques, including FTIR, NMR, and mass spectral analysis.

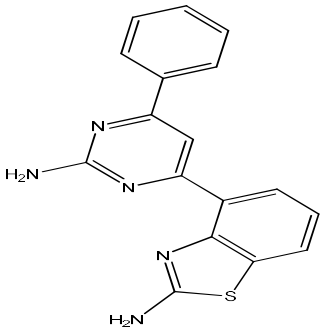

PR 1
Yield: 65%
MP:296-299 °C
M.F: $C_{17}H_{13}N_5S$

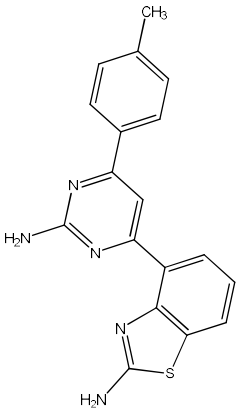

PR 2
Yield: 60%
MP:284-288°C
M.F: $C_{18}H_{15}N_5S$

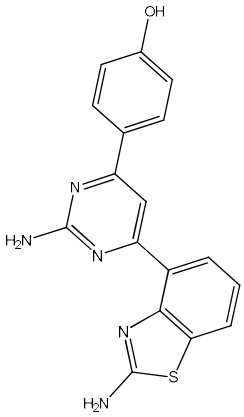

PR 3
Yield: 67%
MP: 296-298°C
M.F: $C_{17}H_{13}N_5OS$

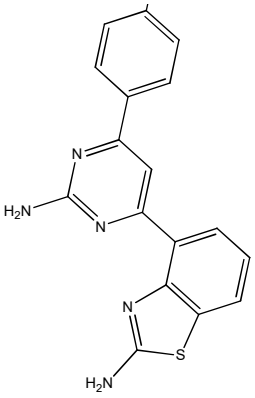

PR 4
Yield: 72%
MP: 309-312°C
M.F: $C_{18}H_{15}N_5OS$

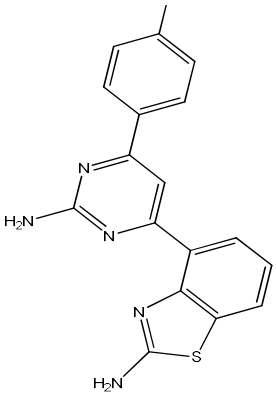

PR 5
Yield: 72%
MP: 285-289°C
M.F: $C_{19}H_{18}N_6S$

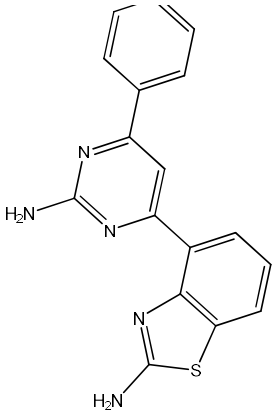

PR 6
Yield: 62%
MP: 291-294°C
M.F: $C_{17}H_{12}N_6O_2S$

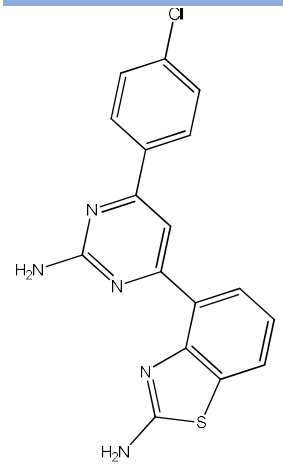

PR 7
Yield: 72%
MP: 262-264ºC
M.F: $C_{17}H_{12}ClN_5S$

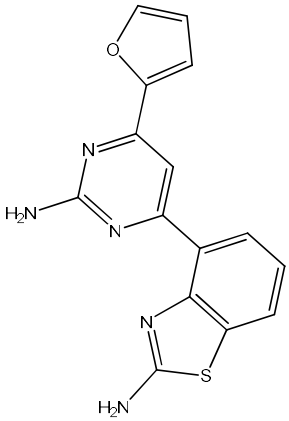

PR 8
Yield: 72%
MP: 236-238ºC
M.F: $C_{15}H_{11}N_5OS$

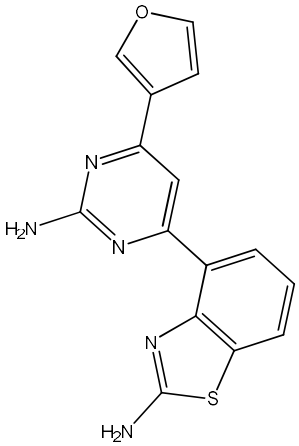

PR 9
Yield: 72%
MP: 242-244 ºC
M.F: $C_{15}H_{11}N_5OS$

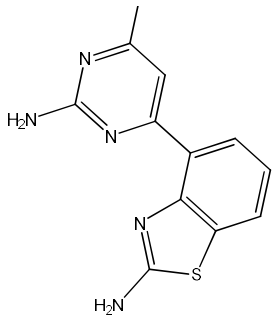

PR 10
Yield: 68%
MP: 264-266ºC
M.F: $C_{15}H_{11}N_5S_2$

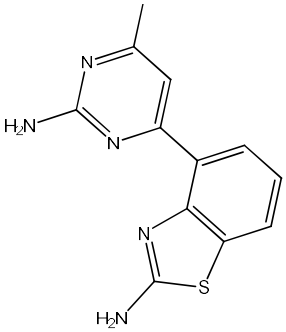

PR 11
Yield: 68%
MP: 286-289ºC
M.F: $C_{15}H_{11}N_5S_2$

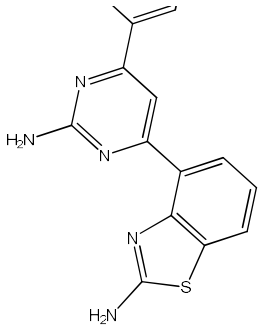

PR 12
Yield: 68%
MP: 292-295ºC
M.F: $C_{16}H_{12}N_6S$

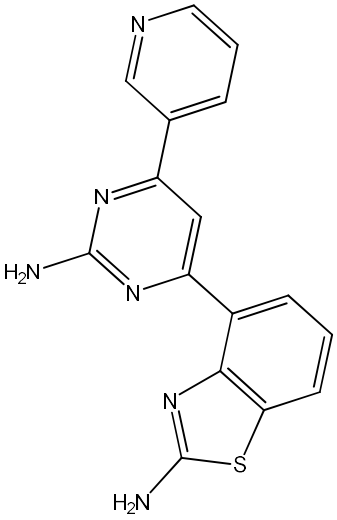

PR 13
Yield: 58%
MP: 310-312ºC
M.F: $C_{16}H_{12}N_6S$

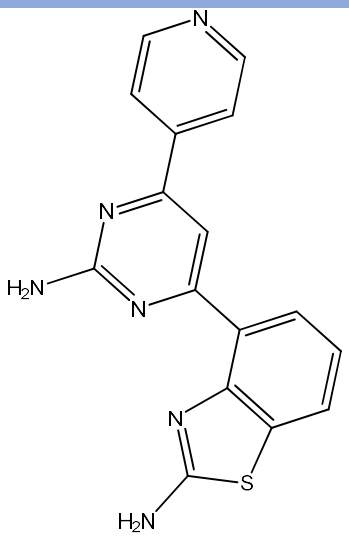

PR 14
Yield: 62%
MP: 310-312ºC
M.F: $C_{16}H_{12}N_6S$

BIOLOGICAL METHOD

The process of reducing MTT (3-(4,5-dimethylthiazol-2-yl)-2,5-diphenyltetrazolium bromide) is a biochemical reaction utilized in laboratory[8] assays to evaluate cellular metabolic activity and viability, serving as the foundation for the MTT assay. MTT, a tetrazolium salt, undergoes reduction by mitochondrial dehydrogenases present in living cells. These enzymes, which play a crucial role in cellular respiration, facilitate the transfer of electrons to MTT, resulting in the formation of a purple formazan product. The extent of this reduction is directly proportional to the number of viable cells, as formazan accumulates within the mitochondria.

During the MTT assay, cells are treated with MTT[9], leading to the formation of formazan crystals. These crystals are then solubilized using a solvent such as dimethyl sulfoxide (DMSO), and the absorbance is measured at a wavelength of 570 nm. The quantity of formazan generated is indicative of the number of viable cells, enabling the assay to evaluate cytotoxicity, cell proliferation, and the impact of various treatments on cell viability[10].

Materials and Methods

Cell Lines and Culture Conditions

HT-29 (colon cancer) and MCF-7[11] (breast cancer) cell lines were sourced from the National Centre for Cell Science (NCCS) located in Pune, India. Dulbecco's Modified Eagle's Medium (DMEM), Minimum Essential Media Eagle (MEM), MTT [3-(4,5-dimethylthiazol-2-yl)-2,5-diphenyltetrazolium bromide], Trypsin, and EDTA were acquired from Sigma Chemicals in St. Louis, Missouri. Fetal bovine serum (FBS) was obtained from Arrow Labs, and 96-well flat-bottom tissue culture plates were procured from Tarson[12].

Preparation of Test Compounds:

Test compounds, such as pharmaceuticals and natural products, were initially dissolved in a solvent, specifically dimethyl sulfoxide[13] (DMSO), to create a stock solution at a concentration of 10 mM. These stock solutions were subsequently diluted in culture medium to obtain the required final concentrations for the assay[14].

MTT Assay Procedure:

1. Cell Seeding: HT-29 and MCF-7 cell lines were plated in 96-well plates at a density of 5,000 to 10,000 cells per well and incubated for 24 hours at 37°C in an atmosphere containing 5% CO_2.

2. Treatment: Following the incubation period, the cells were exposed to serial dilutions of the test compound for durations of 24, 48, or 72 hours. Control wells were treated with the vehicle solvent (DMSO, at a concentration of less than 1%).

3. MTT Addition: Upon completion of the treatment period, 20 µL of MTT solution (5 mg/mL) was introduced to each well and incubated for 4 hours at 37°C, during which viable cells converted MTT into purple formazan.

4. Formazan Solubilization: The culture medium was removed, and 150 µL of DMSO or an appropriate solubilizing solution was added to dissolve the formazan crystals. The plate was then shaken for 10 minutes to ensure complete solubilization.

5. Absorbance Measurement: The absorbance[16] was recorded at 570 nm using a microplate reader, with background absorbance at 630 nm being subtracted from the readings.

Toxicity Assessment and Interpretation:

- **Cytotoxicity**: Compounds causing significant reduction in cell viability were considered cytotoxic.
- **IC_{50} Determination**: The IC_{50} values (concentration inhibiting 50% of cell viability) were calculated using nonlinear regression analysis, indicating the potency of compounds[15].

% inhibition= ((control value- sample value)/ control value) * 100

IC_{50}=Inv.log (50-c)/m; c and m derived from y= mx+c of plot of % inhibition Vs log C.

In Vitro Antitubercular Activity:

The in vitro antitubercular activity of compounds was tested using *Mycobacterium tuberculosis* H37Rv. This strain is a reference for studying tuberculosis[17] and testing antitubercular compounds

due to its well-characterized properties. The effectiveness of compounds was assessed by their ability to inhibit Mtb growth in controlled laboratory conditions.

Molecular Docking Studies

Ligand-protein inverse docking (LPID) is a valuable method in drug design used to identify potential ligands by docking small molecules to receptor sites in various conformations[18]. Advanced docking algorithms like multi-conformer shape matching, genetic algorithms, and simulated annealing help accurately predict ligand-receptor interactions[25]. This approach aids in discovering new and secondary therapeutic targets for drugs, natural products, and other ligands.

In this study, computational tools such as ArgusLab for energy minimization, Accelrys Draw for molecular modeling, and iGEMDOCK for docking simulations were used to evaluate the PR1-PR-14 compound series against anticancer and antitubercular targets[19]. The goal was to analyze binding energies, interactions, and modes of the ligands within target active sites. The iGEMDOCK software requires ligand and receptor coordinates in PDB or Mol-2 formats, with non-polar hydrogen atoms transferred and receptor files cleaned. Crystallographic ligands from X-ray structures helped identify binding sites for docking[20].

Anticancer Activity:

The synthesized benzothiazole-linked chalcones (CH-1-CH-14) target cyclin-dependent kinase 2 (CDK2) and histone deacetylase (HDAC), both important in the development of colon and breast cancers[21].

Anti-Tubercular Activity:

Isoniazid (INH) targets the enzymes InhA and 8an5, which are critical in the fatty acid biosynthesis pathway of *Mycobacterium tuberculosis*. INH inhibits InhA and may also affect 8an5, disrupting mycolic acid synthesis and hindering bacterial cell wall formation[22].

RESULTS OF CYTOTOXICITY STUDIES

Table 1.1: Cytotoxicity data of benzothiazole-linked pyrimidines PR1-PR14 against HT-29 colon cancer cell line**.**

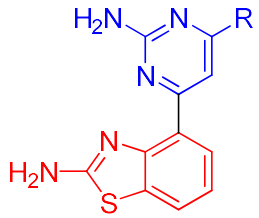

Compound Code	R	IC_{50} (µg/mL) (Mean ± SEM)
PR1	C_6H_5	48.16 ± 0.1
PR2	4-MeC_6H_4	32.06 ± 0.2
PR3	4-OHC_6H_4	5.13 ± 0.9
PR4	4-$OMeC_6H_4$	20.11 ± 0.9
PR5	4-$NMe_2C_6H_4$	25.17 ± 0.1
PR6	4-$NO_2C_6H_4$	57.12 ± 0.1

PR7	4-ClC_6H_4	8.27 ± 0.9
PR8	Furan-2-yl	59.07 ± 0.1
PR9	Furan-3-yl	89.10 ± 0.1
PR10	Thiophen-2-yl	11.13 ± 0.3
PR11	Thiophen-3-yl	75.57 ± 0.1
PR12	Pyridin-2-yl	59.48 ± 0.1
PR13	Pyridin-3-yl	67.07 ± 0.3
PR 14	Pyridin-4-yl	26.28 ± 0.1
Methotrexate	-	0.8 ± 0.5

Table 1.2: Cytotoxicity data of benzothiazole-linked pyrimidines PR1-PR14 against MCF-7 breast cancer cell line**.**

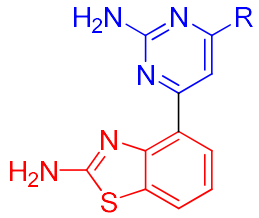

Compound Code	**R**	**IC_{50} (µg/mL) (Mean ± SEM)**
PR1	C_6H_5	43.01 ± 0.1
PR2	4-MeC_6H_4	41.18 ± 0.2
PR3	4-OHC_6H_4	83.04 ± 0.3
PR4	4-$OMeC_6H_4$	23.07 ± 0.9
PR5	4-$NMe_2C_6H_4$	45.07 ± 0.7
PR6	4-$NO_2C_6H_4$	16.01 ± 0.9
PR7	4-ClC_6H_4	27.15 ± 0.3
PR8	Furan-2-yl	31.01 ± 0.1
PR9	Furan-3-yl	51.07 ± 0.4
PR10	Thiophen-2-yl	11.07 ± 0.1
PR11	Thiophen-3-yl	59.07 ± 0.9
PR12	Pyridin-2-yl	06.06 ± 0.1
PR13	Pyridin-3-yl	66.01 ± 0.4
PR 14	Pyridin-4-yl	48.08 ± 0.1
Methotrexate	-	2.8 ± 0.3

Table 1.3: The inhibitory activity data of benzothiazole-linked pyrimidines PR1-PR14 against *Mycobacterium tuberculosis* H37Rv.

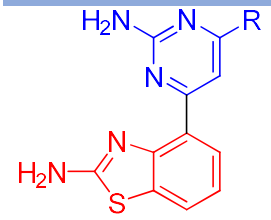

S.No	Compound Code	R	MIC values (µg/mL) of M. tuberculosis $H_{37}Rv$
1	PR 1	C_6H_5	100
2	PR 2	4-MeC_6H_4	50
3	PR 3	4-OHC_6H_4	50
4	PR 4	4-$OMeC_6H_4$	25
5	PR 5	4-$NMe_2C_6H_4$	50
6	PR 6	4-$NO_2C_6H_4$	6.25
7	PR 7	4-ClC_6H_4	50
8	PR 8	Furan-2-yl	6.25
9	PR 9	Furan-3-yl	100
10	PR 10	Thiophen-2-yl	50
11	PR 11	Thiophen-3-yl	100
12	PR 12	Pyridin-2-yl	12.5
13	PR 13	Pyridin-3-yl	50

S.No	Compound Code	R	MIC values (µg/mL) of M. tuberculosis $H_{37}Rv$
14	PR 14	Pyridin-4-yl	100
15	Pyrazinamide	--	3.125

Table 1.4: Benzothiazole-linked pyrimidines PR 1-PR-14 Their GEMDOCK scores in relation to validated anticancer protein drug targets.

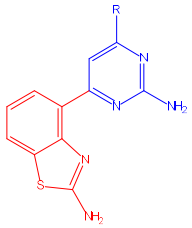

Compound	R	CDK2	HDAC
		GEMDOCK Score	GEMDOCK Score
		kcal/mol	kcal/mol
PR 1	C_6H_5	-79.920	-97.473
PR 2	4-MeC_6H_4	-97.610	-101.537
PR 3	4-OHC_6H_4	-91.333	-111.579
PR 4	4-$OMeC_6H_4$	-96.810	-114.651
PR 5	4-$NMe_2C_6H_4$	-94.252	-103.330
PR 6	4-$NO_2C_6H_4$	**-141.201**	**-148.212**

PR 7	4-ClC_6H_4	-104.216	-100.880
PR 8	Furan-2-yl	-91.313	-102.991
PR 9	Furan-3-yl	-94.112	-100.748
PR 10	Thiophen-2-yl	-100.510	-116.361
PR 11	Thiophen-3-yl	-104.100	-129.253
PR 12	Pyridin-2-yl	-94.801	-107.828
PR 13	Pyridin-3-yl	-94.582	-88.432
PR 14	Pyridin-4-yl	-86.505	-113.616

Table 1.5: Benzothiazole-linked pyrimidines PR-1-PR-14 Their GEMDOCK scores in relation to validated antitubercular protein drug targets.

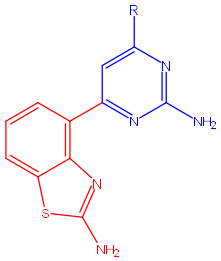

Compound	**R**	**InhA**
		GEMDOCK Score
		kcal/mol
PR-1	C_6H_5	-90.623
PR-2	4-MeC_6H_4	-109.158
PR-3	4-OHC_6H_4	**-117.653**
PR-4	4-$OMeC_6H_4$	-92.101
PR-5	4-$NMe_2C_6H_4$	-92.052
PR-6	4-$NO_2C_6H_4$	-92.638

PR-7	4-ClC_6H_4	-95.581
PR-8	Furan-2-yl	-93.017
PR-9	Furan-3-yl	-90.852
PR-10	Thiophen-2-yl	-95.071
PR-11	Thiophen-3-yl	-101.181
PR-12	Pyridin-2-yl	-89.606
PR-13	Pyridin-3-yl	-89.964
PR-14	Pyridin-4-yl	-79.363

DISCUSSION ON THE RESULTS

The analysis of the inhibitory activity data for the in vitro HT-29 colon cancer cell line (Table 1.1) indicated that the compounds PR3, PR7, PR10, and PR4 exhibited the most significant inhibitory effects, with IC50 values of 5.13 ± 0.9, 8.27 ± 0.9, 11.13 ± 0.3, and 20.11 ± 0.9 µg/mL, respectively. Notably, compounds PR5 and PR14 also demonstrated considerable inhibitory activity, with IC50 values of 25.17 ± 0.1 and 26.28 ± 0.1 µg/mL, respectively. The compound PR2 displayed a moderate level of activity, with an IC50 value of 32.01 ± 0.8 µg/mL. In contrast, compounds PR1, PR6, PR8, PR12, PR13, PR11, and PR9 showed relatively lower activity, with IC50 values ranging from 48.17 ± 0.1 to 89.10 ± 0.1 µg/mL, particularly when compared to the standard drug Methotrexate, which has an IC50 of 0.8 ± 0.5 µg/mL. The Structure-Activity Relationship (SAR) analysis of these compounds clearly illustrated the key role of the basic nucleus, comprising benzothiazole and pyrimidine moieties, in the inhibitory activity against the HT-29 colon cancer cell line, as observed in compounds PR1-PR14. In certain instances, the presence of specific substituents enhanced the activity, while others diminished it.PR3 (4-OHC_6H_4)>PR7 (4-ClC_6H_4)>PR10 (Thiophen-2-yl)>PR4 (4-$OMeC_6H_4$)>PR5 (4-$NMe_2C_6H_4$)>PR14 (Pyridin-4-yl)>PR2 (4-MeC_6H_4)>PR1 (C_6H_5)>PR6 (4-$NO_2C_6H_4$)>PR8 (Furan-2-yl)>PR12 (Pyridin-2-yl)>PR13 (Pyridin-3-yl)>PR11 (Thiophen-3-yl)>PR9 (Furan-3-yl). However, it was revealed that various aliphatic/aromatic/heteroaromatic functional group substitutions on pyrimidine ring system followed its activity order as PR3 (4-OHC_6H_4, IC_{50}: 5.13 ± 0.9 µg/mL)>PR7 (4-ClC_6H_4, IC_{50}: 8.27 ± 0.9 µg/mL)>PR10 (Thiophen-2-yl, IC_{50}: 11.13 ± 0.3 µg/mL)>PR4 (4-$OMeC_6H_4$, IC_{50}: 20.11 ± 0.9 µg/mL)>PR5 (4-$NMe_2C_6H_4$, IC_{50}: 25.17 ± 0.1 µg/mL)>PR14 (Pyridin-4-yl, IC_{50}: 26.28 ± 0.1 µg/mL)>PR2 (4-MeC_6H_4, IC_{50}: 32.07 ± 0.2 µg/mL)>PR1 (C_6H_5, IC_{50}: 48.17 ± 0.1 µg/mL)>PR6 (4-$NO_2C_6H_4$, IC_{50}: 57.12 ± 0.1 µg/mL)>PR8 (Furan-2-yl, IC_{50}: 59.07 ± 0.1 µg/mL)>PR12 (Pyridin-2-yl, IC_{50}: 59.48 ± 0.1 µg/mL)>PR13 (Pyridin-3-yl, IC_{50}: 67.07 ± 0.3 µg/mL)>PR11 (Thiophen-3-yl, IC_{50}: 75.57 ± 0.1 µg/mL)>PR9 (Furan-3-yl, IC_{50}: 89.10 ± 0.1 µg/mL), respectively.

The analysis of the inhibitory activity screening data for the in vitro MCF-7 breast cancer cell line (Table 1.2) indicated that the compounds PR12 and PR10 exhibited the most significant inhibitory effects, with IC50 values of 06.06 ± 0.1 and 11.07 ± 0.1 µg/mL, respectively. Notably, compounds PR6 and PR4 also demonstrated considerable inhibitory activity, presenting IC50 values of 16.01 ± 0.9 and 23.07 ± 0.9 µg/mL, respectively. In contrast, compounds PR7 and PR8 displayed moderate activity levels, with IC50 values of

27.15 ± 0.3 and 31.01 ± 0.1 µg/mL. The remaining compounds, including PR2, PR1, PR5, PR14, PR9, PR11, PR13, and PR3, showed relatively lower activity, with IC50 values ranging from 41.18 ± 0.2 to 83.04 ± 0.3 µg/mL, particularly when compared to the standard drug Methotrexate, which has an IC50 of 2.8 ± 0.3 µg/mL. The Structure-Activity Relationship (SAR) analysis of these compounds clearly illustrated the inherent characteristics of the MCF-7 breast cancer cell line inhibitory activity, which is associated with the fundamental structure comprising benzothiazole and pyrimidine moieties, as observed in compounds PR1-PR14. In certain instances, the activity was enhanced by specific substituents, while in others, it was diminished by different substituents.PR12 (Pyridin-2-yl)>PR10 (Thiophen-2-yl)>PR6 (4-$NO_2C_6H_4$)>PR4 (4-$OMeC_6H_4$)>PR7 (4-ClC_6H_4)>PR8 (Furan-2-yl)>PR2 (4-MeC_6H_4)>PR1 (C_6H_5)>PR5 (4-$NMe_2C_6H_4$)>PR14 (Pyridin-4-yl)>PR9 (Furan-3-yl)>PR11 (Thiophen-3-yl)>PR13 (Pyridin-3-yl)>PR3 (4-OHC_6H_4). However, it was revealed that various aliphatic/aromatic/heteroaromatic functional group substitutions on pyrimidine ring system followed its activity order as PR12 (Pyridin-2-yl, IC_{50}: 06.06 ± 0.1 µg/mL)>PR10 (Thiophen-2-yl, IC_{50}: 11.07 ± 0.1 µg/mL)>PR6 (4-$NO_2C_6H_4$, IC_{50}: 16.01 ± 0.9 µg/mL)>PR4 (4-$OMeC_6H_4$, IC_{50}: 23.07 ± 0.9 µg/mL)>PR7 (4-ClC_6H_4, IC_{50}: 27.15 ± 0.3 µg/mL)>PR8 (Furan-2-yl, IC_{50}: 31.01 ± 0.1 µg/mL)>PR2 (4-MeC_6H_4, IC_{50}: 41.18 ± 0.2 µg/mL)>PR1 (C_6H_5, IC_{50}: 43.01 ± 0.1 µg/mL)>PR5 (4-$NMe_2C_6H_4$, IC_{50}: 45.07 ± 0.7 µg/mL)>PR14 (Pyridin-4-yl, IC_{50}: 48.08 ± 0.1 µg/mL)>PR9 (Furan-3-yl, IC_{50}: 51.07 ± 0.4 µg/mL)>PR11 (Thiophen-3-yl, IC_{50}: 59.07 ± 0.9 µg/mL)>PR13 (Pyridin-3-yl, IC_{50}: 66.01 ± 0.4 µg/mL)>PR3 (4-OHC_6H_4, IC_{50}: 83.04 ± 0.3 µg/mL), respectively.

The analysis of the in vitro inhibitory activity screening data for Mycobacterium tuberculosis H37Rv (Table 1.3) indicated that the compounds PR6 and PR8 exhibited the highest levels of inhibitory activity, both demonstrating values of 6.25 µg/mL. Notably, the compound PR12 also displayed significant inhibitory effects, with a value of 12.5 µg/mL. In contrast, the compound PR4 showed a moderate level of activity at a concentration of 25 µg/mL. The compounds PR2, PR3, PR5, PR7, PR10, and PR13 exhibited activity at concentration values of 50 µg/mL. Meanwhile, compounds PR1, PR9, PR11, and PR14 demonstrated relatively lower activity, with IC50 values of 100 µg/mL, especially when compared to the standard drug Pyrazinamide, which has an IC50 of 3.125 µg/mL. The Structure-Activity Relationship (SAR) analysis of these compounds clearly illustrated the inherent characteristics of the inhibitory activity against Mycobacterium tuberculosis H37Rv, which is associated with the fundamental structure comprising benzothiazole and pyrimidine moieties, as observed in compounds PR1 through PR14.

A collection of 14 benzothiazole-linked pyrimidines, designated as PR1-PR14, underwent ligand-protein inverse induced fit docking simulations utilizing the iGEMDOCK version 2.1 software. These compounds were evaluated against the validated drug targets CDK2 and HDAC. The findings, as presented in Table 1.4, may facilitate the preliminary identification of potential target-based hits (best fit) in relation to the observed cytotoxicity. The identification of the hit (best fit molecule) for each target was determined by analyzing its binding energy and interactions within the active binding sites. According to the results from LPID studies on the benzothiazole-linked pyrimidines PR1-PR14, compound PR-6 demonstrated a stable binding phenomenon with the lowest binding energy of -141.201 kcal/mol against the CDK2 protein drug target. Similarly, compound PR-6 exhibited the least binding energy and the most stable binding orientation within the active binding site region of HDAC, recorded at -148.212 kcal/mol.

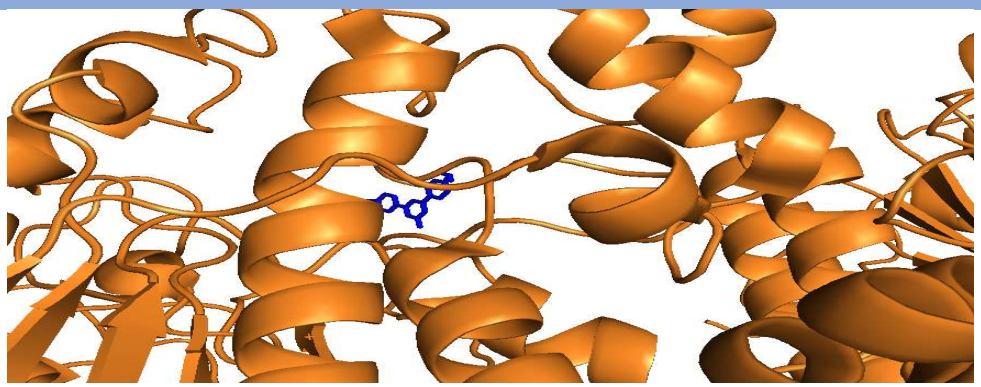

Active binding site, binding mode and H-bond interactions of PR-6 against HDAC.

A set of 14 benzothiazole-linked pyrimidines PR-1-PR-14 were subjected to ligand-protein inverse induced fit docking simulation using software iGEMDOCK version 2.1. These compounds were docked against validated InhA drug target. The results **(Table 1.5)** of this simulation could help in preliminary identification of potential target based hit (best fit) with respect to the observed anti-tubercular activity[26] . The hit (best fit molecule) identified against InhA target was based on its binding energy and binding interactions with in the active binding site. From the results of LPID studies on benzothiazole-linked pyrimidinesPR-1-PR-14the compound **PR-3**showedstable binding phenomenon with least binding energy at **-117.653 kcal/mol** against InhA protein drug target.

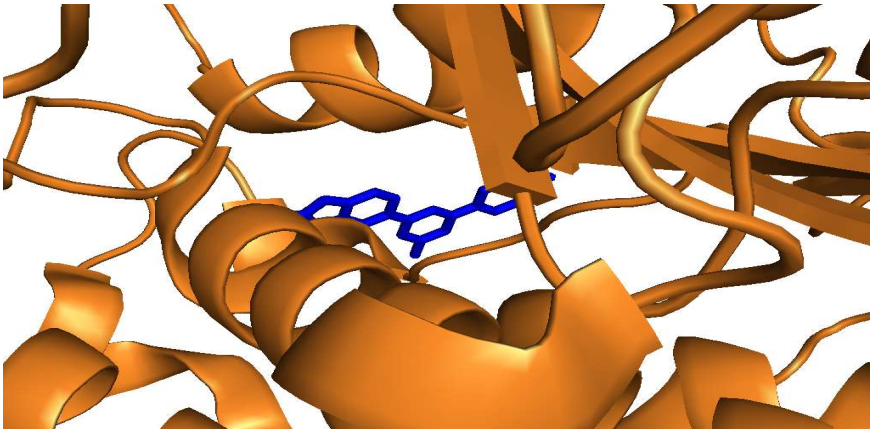

Active binding site, binding mode and H-bond interactions of PR-3 against InhA.

A set of 14 benzothiazole-linked pyrimidines PR-1-PR-14 were subjected to ligand-protein inverse induced fit docking simulation using software iGEMDOCK version 2.1. These compounds were docked against validated InhA drug target[27]. The results **(Table 1.5)** of this simulation could help in preliminary identification of potential target based hit (best fit) with respect to the observed anti-tubercular activity. The hit (best fit molecule) identified against InhA target was based on its binding energy and binding interactions[28] with in the active binding site. From the results of LPID studies on benzothiazole-linked pyrimidines PR-1-PR-14 the compound **PR-4** showedstable binding phenomenon with least binding energy at **-98.221 kcal/mol** against InhA protein drug target.

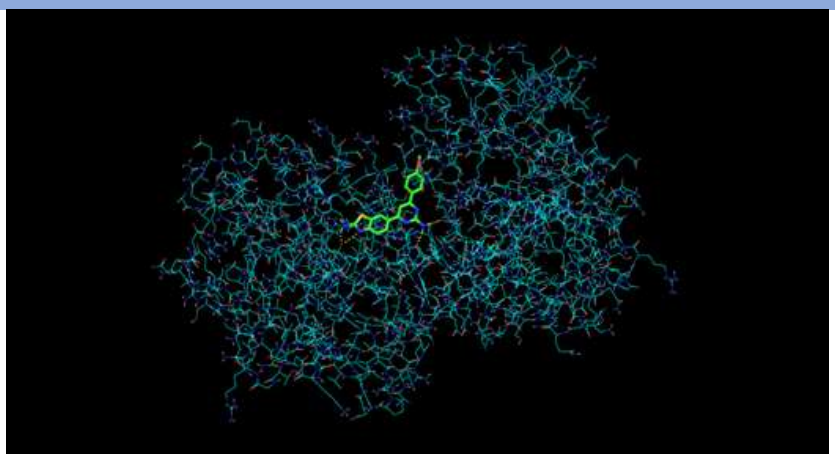

Active binding site, binding mode and H-bond interactions of PR-4 against protein 8an5 (sticks).

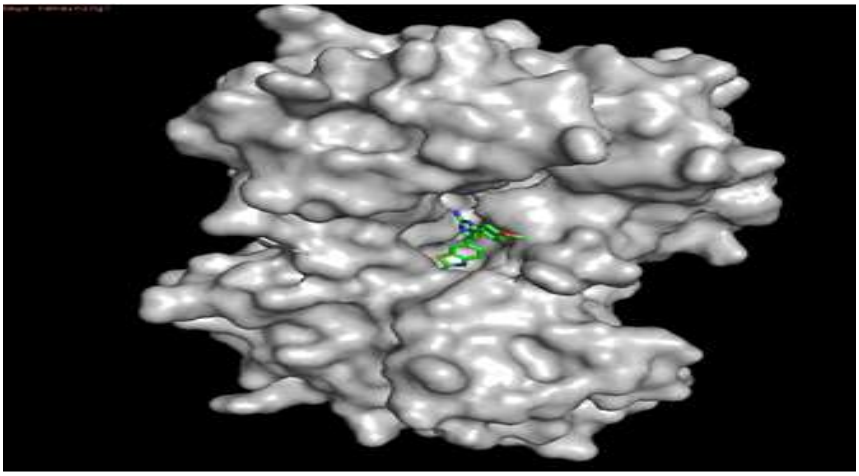

Active binding site, binding mode and H-bond interactions of PR-4 against protein 8an5 surface-1.

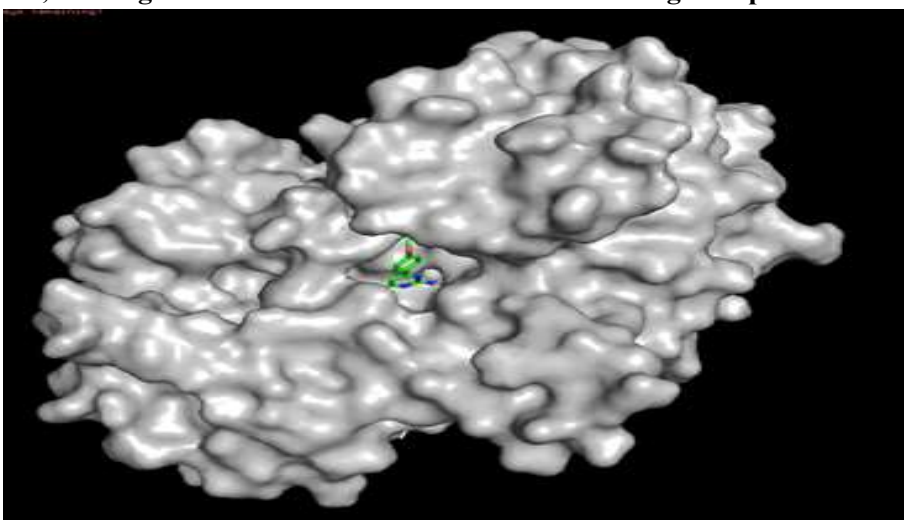

Active binding site, binding mode and H-bond interactions of PR-4 against protein 8an5 surface-2.

References

1. Maayan, S.; Ohad, N. and Soliman, K.;Bioorg. Med. Chem.;2005, 13, 433.
2. Nowakowska, Eur. J. Med. Chem.;2007, 42, 125.

3. Go, M.L.; Wu, X. and Liu, X.L.; Current Medicinal Chemistry, 2005, 12,483.
4. Mark, C. and Nagarathnam, D.; J. Nat. Prod.;1991, 54, 1656.
5. Anjaneyulu, A.S.R.; Sudha Rani, G.; Mallavadhani, U.V. and Murthy, Y.L.N.; Ind. J. Het. Chem.; 1994, 4, 9.
6. Bukhari, S. N. A.; Jasamai, M.; Jantan, I. Mini Reviews in Medicinal Chemistry 2012, 12 (13), 1394-1403.
7. Wilson, A.P., in: Cytotoxicity and viability assays: In JRW Masters, "Animal Cell Culture", 3rd ed., Oxford University, Oxford, 1, 175 (2000).
8. Maria C. S. L., Marcus, V. N., Alessandra, C. P., Marcelle, L. F., Goncalves, T, M., Nogneira, M. A. P. Arkivoc, 15, 181 (2007).
9. Banerjee, A.; Dubnau, E.; Quemard, A.; Balasubramanian, V.; Um, K. S.; Wilson, T.; Collins, D.; de Lisle, G.; Jacobs, W. R. Science. 1994, 263, 227.
10. Dessen, A.; Quemard, A.; Blanchard, J. S.; Jacobs, W. R. Science. 1995, 267, 1638.
11. Heitsch, H.; Becker, A. H. R.; Kleemann, W. H.; Wagner, A.Bioorg. Med. Chem. 1997, 5, 673.
12. Salamon, E.; Mannhold, R.; Weber, H.; Lemoine, H.; Frank, W. J. Med. Chem. 2002,45, 1086.
13. Choi, J. K.; Noh, M. K., Choi, D. J.; Park, S. J.; Won, S. H.; Kim, R. J.; Kim, S. J.; Yoon, M. Y. Bull. Korean Chem. Soc. 2006, 10, 1697.
14. Makrandi, J.K. and Kumar, S.;Asian J. Chem.;2004, 16, 1189.
15. Baviskar, B.; Patel, S.; Baviskar, B.; Khadabadi, S. S. and Shiradkar, M.; Asian J. Research Chem.;2008, 1, 67.
16. Karthikeyan, M.S.; Shivarama, B.H. and SuchethaKumari, N.; Eur. J. Med. Chem.;2007, 42, 30.
17. Tsukiyama, R.I.; Katsura, H.; Tokuriki, N. and Kobayashi, M.; Antimicrobial Agents Chemother.;2002, 46, 1226.
18. More, A. H. and Ramaa, C. S.;Ind. J. Chem.;2010, 49, 364.
19. Lee, H.U., Kim, B.Y., Ahn, J.B., Kang, S.K., Lee, .J.H., Shin, J.S., Ahn, S.K., Lee, S.J. and Yoon, Z.S., Eur. J. Med. Chem., 40, 862 (2005).
20. Burger, A., in: Burger's Medicinal Chemistry and drug discovery, John Wiley publications inc. 5th edition. (1995).
21. Maria C. S. L., Marcus, V. N., Alessandra, C. P., Marcelle, L. F., Goncalves, T, M., Nogneira, M. A. P. Arkivoc, 15, 181 (2007).
22. Hollander, J.N.D., J. Clin.Lab.Anal., 10, 42 (1996).
23. Ibrahim DA, El-Metwally AM. Design, synthesis, and biological evaluation of novel pyrimidine derivatives as CDK2 inhibitors. European journal of medicinal chemistry. 2010 Mar 31;45(3):1158-66.
24. Orlikova B, Tasdemir D, Golais F, Dicato M, Diederich M. Dietary chalcones with chemopreventive and chemotherapeutic potential. Genes & nutrition. 2011May 1;6(2):125-47.
25. Thanh Tung T, Thi Kim Oanh D, Thi Phuong Dung P, Thi My Hue V, Ho Park S, Woo Han B, Kim Y, Hong JT, Han SB, Nam NH. New benzothiazole/thiazole-containing hydroxamic acids as potent histone deacetylase inhibitors and antitumor agents. Medicinal Chemistry. 2013 Dec 1;9(8):1051-7.
26. Rogers, D.; Hopfinger, A.J. Application of genetic functionl approximation to quantitative structure-activity relationships and quantitative structure-property relationships. J. Chem. Inf. Comput. 30 Sci.1994, 34, 854.
27. Vilchèze C, Baughn AD, Tufariello J, Leung LW, Kuo M, Basler CF, Alland D, Sacchettini JC, Freundlich JS, Jacobs WR. Novel inhibitors of InhA efficiently kill Mycobacterium tuberculosis under aerobic and anaerobic conditions. Antimicrobial agents and chemotherapy. 2011 Aug 1;55(8):3889-98.